Niobium for High Temperature Applications
Edited by Young-Won Kim and Tadeu Carneiro
TMS (The Minerals, Metals & Materials Society), 2004

FRACTURE AND FATIGUE OF Nb ALLOYS AND COMPOSITES

John J. Lewandowski

Department of Materials Science and Engineering
Case Western Reserve University
Cleveland, Ohio 44106-7204

Keywords: Fracture, Fatigue, Nb-Silicides, Bulk Glass Composites

Abstract

The flow and fracture of engineering materials is controlled by microstructural features as well as the imposed stress state. This paper reviews ongoing work on a number of Nb based systems where the effects of systematic changes in microstructure and stress state on the flow, fracture, and fatigue behavior are being determined. Experiments utilizing notched and fatigue precracked specimens, as well as smooth specimens tested over a range of temperatures from 77K to 773K are described. In-situ fracture experiments conducted inside a scanning electron microscope are also described in order to delineate the sequence of deformation and fracture events occurring in both intermetallic and metallic glass composites, which utilize Nb or a Nb phase as a toughening constituent. In particular, Nb-Nb Silicide composites will be covered and a comparison to the behavior of some other high temperature systems will be provided to highlight some of the potential benefits and problems provided by using Nb/Nb alloys as a toughening constituent. The paper concludes with a summary of more recent work where Nb/Nb alloys have been used to beneficially change the properties of bulk metallic glasses.

Introduction

The potential use of alloys and intermetallic composites based on refractory metals continues to receive attention for some of the highest temperature structural applications [1-3]. In addition, recent investigations have also revealed the benefits of using Nb/Nb alloys in bulk metallic glasses, where improvements in tensile ductility, fracture toughness, and impact toughness are possible via composite approaches which utilize Nb/Nb alloys as one constituent [4-8].

Although the oxidation resistance of monolithic refractory metals are generally poor, and could limit their use at high temperatures, the intermetallic compounds of refractory metals with silicon (e.g. Nb, Mo) are of interest because of their high melting points, their increased oxidation resistance, and their relatively low densities [1-3]. In particular, alloys/composites in the systems Mo-Si-B -X (X = W, V, Cr, Nb, Al, Ge, Re) and Nb-Ti-Hf-Cr-Al-Si-Ge combine many of the attractive features of refractory metals and intermetallic compounds. Despite the potential of silicides for use as high temperature materials such as turbine airfoils or some hypersonic applications for service temperatures ranging from 1000-1400^{o}C, relatively little is known about their structure and properties (in monolithic or composite form) at ambient or elevated temperatures. Some of the property requirements for the hottest parts of aircraft engines are provided elsewhere [2,3].

Predominant issues in the mechanical behavior of these advanced refractory based materials are their ambient and high temperature properties, including the strength, ductility, toughness, creep, and fatigue performance, while the oxidation resistance at intermediate and high temperatures is also under investigation. Recent works have successfully demonstrated the potential of improving the toughness of niobium silicide systems via compositing with ductile Nb phases utilizing ingot casting and extrusion, directional solidification, as well as lamination via PVD or powder metallurgy techniques [1-3,9-11]. Parallel efforts are being developed to improve the oxidation and creep resistance of Nb via alloying without compromising the toughness. Much less is known about the effects of such alloying on creep, and in particular, the fatigue behavior of the niobium silicide based system.

In the case of metallic glass composites, the introduction of Nb containing phase(s) in the metallic glass has been shown to increase the tensile ductility, fracture toughness, and impact toughness [4-8]. However, the exact mechanisms controlling this behavior have not been determined, while the structures have not been optimized yet for a complete balance of properties. It appears that the tough and ductile Nb phase(s) are effective in dispersing the intense localized shear characteristic of amorphous metals, thereby producing enhanced tensile ductility as well as impact toughness.

The flow, fracture, and fatigue performance of the toughened Nb silicide based composites, as well as the composite metallic glasses are significantly affected by the flow, fracture, and fatigue performance of the toughening phase. In most of the composite systems studied to date, the Nb toughening phase contains additional alloying elements, either due to contamination (e.g. O, C, etc.) or due to alloying (e.g. Si, Hf, Ti, Cr, Ge, Zr, etc.) to improve the oxidation resistance and/or other properties. In order to be able to document the effects of toughening phase(s) on the composite behavior, it is necessary to understand the effects of microstructural changes on the flow, fracture, and fatigue performance of the toughening phase itself. This paper will first review the available literature on the factors which control the flow, fracture, and fatigue behavior of Nb and Nb alloys. The effects of microstructural changes on the behavior of polycrystalline Nb will be covered first, followed by recent fracture and fatigue studies over temperatures ranging from 77K – 773K on Nb toughened Nb silicide composites prepared either by arc casting/extrusion or directional solidification (DS). The behavior of metallic glasses toughened via a Nb containing phase will also be covered. The presence of the silicide intermetallic or metallic glass in the composite will produce constrained flow and elevated tensile stresses in the Nb phase(s), thereby changing the fracture behavior in the Nb toughening phase. The behavior of unconstrained and constrained Nb will be presented for a range of temperatures prior to the discussion of the composite behavior. Test temperatures as low as 77K will be covered as this should illustrate the effects of changes in stress state and flow behavior on the flow/fracture of the toughening phase itself.

Polycrystalline Nb Flow and Fracture Behavior

The flow stress of polycrystalline Nb and its alloys are relatively insensitive to changes in grain size over the range 5 μm to roughly 500 μm. Figure 1 presents a compilation [12,13] of 0.2% offset yield strength data over a range of temperatures and grain sizes taken from the literature as well as from work conducted at CWRU. It is clear that relatively minor increases in strength result from significant changes in the grain size. The Hall-Petch slope obtained for changes in grain size ranging from 20 μm to roughly 165 μm was 8.7×10^4 N/m $^{-3/2}$ [12], consistent with previous work on polycrystalline Nb [14-16] shown in Figure 1. The Ultimate Tensile Stress (UTS) is also relatively insensitive to changes in grain size as shown in Figure 2 [12], taken from a number of other works [14-16].

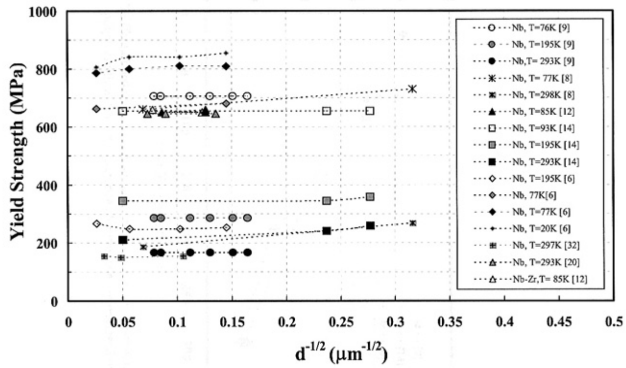

Figure 1. Effects of changes in grain size on yield strength of polycrystalline Nb and Nb alloys [5,13].

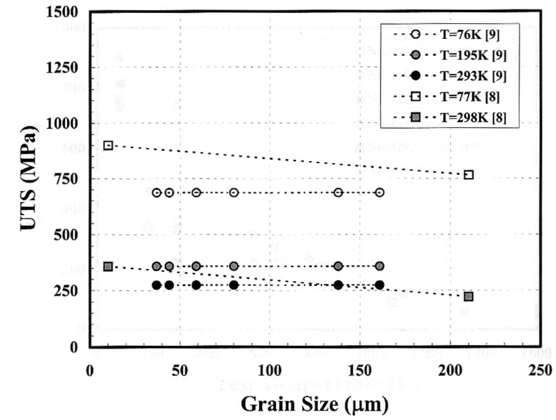

Figure 2. Effects of changes in grain size on UTS of polycrystalline Nb and Nb alloys [5,13].

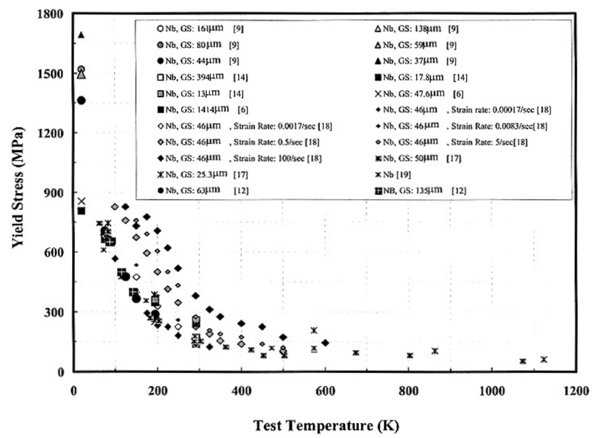

Figure 3. Effects of changes in test temperature on yield stress of Nb and Nb alloys [5,13].

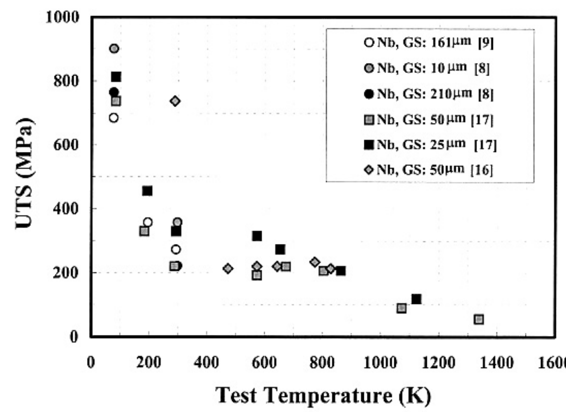

Figure 4. Effects of changes in test temperature on UTS of polycrystalline Nb and Nb alloys [22].

Figures 3 and 4 show the effects of changes in test temperature on the yield stress and UTS, respectively [12-16]. The strength of commercial purity Nb at 298K is 150-300 MPa and at 77K can exceed 1 GPa, while still exhibiting significant ductility and ductile fracture [12-16]. Nb with solid solution additions of Si is significantly strengthened, with strengths at 298K exceeding 350 MPa while still possessing some ductility [11,16,17]. Reductions in test temperature to 77K further increase the yield strength to near 1 GPa, although the fracture at 77K occurs via cleavage with low ductility [11,16,17]. The strength of commercial purity Nb is quite low at high temperatures, while Figure 5 shows the increase in strength obtained for the Nb-Ti-Cr-Al system over a range of temperatures [3,18-21]. Some of the Nb silicide based composites are also shown in Figure 5 and illustrate that strengths approaching 1 GPa at 298K are possible, with high temperature strengths well in excess of that of the monolithic toughening phase [18-21].

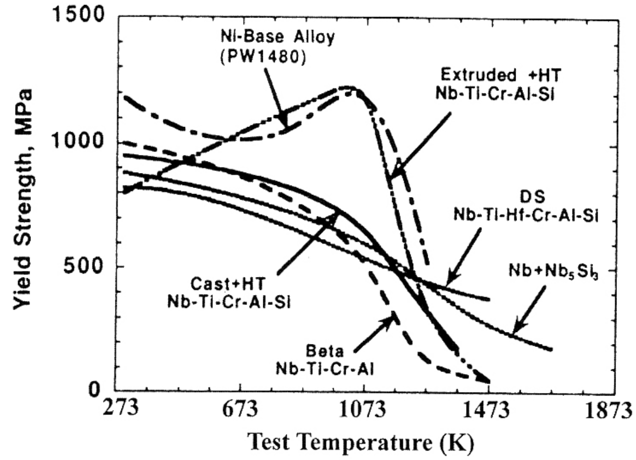

Figure 5. Effects of test temperature on strength of monolithic Nb alloys and Nb Silicide composites [18-21].

The Ductile to Brittle Transition Temperature (DBTT) of polycrystalline Nb is dependent on processing condition and chemistry as well as grain size. Literature data summarized in Figure 6 [12] reveals an effect of processing condition as well as grain size on both the DBTT as well as the notched impact energy. Decreases in grain size reduce the DBTT and increase the impact energy, while high purity Nb prepared via electron beam melting (EBM) exhibited the lowest DBTT and highest notched impact energy for the conditions reported in Figure 6 [12]. Work conducted at CWRU on commercial purity Nb heat treated to different grain sizes similarly reveals an effect of grain size on the DBTT, Figure 7 [22], which shows the amount of brittle (i.e. cleavage) vs. ductile (i.e. non-cleavage) fracture present on fractured impact specimens tested at different temperatures. For example, at 248K, coarse grained Nb exhibited 75% cleavage fracture while the fine grained Nb exhibited 0% cleavage.

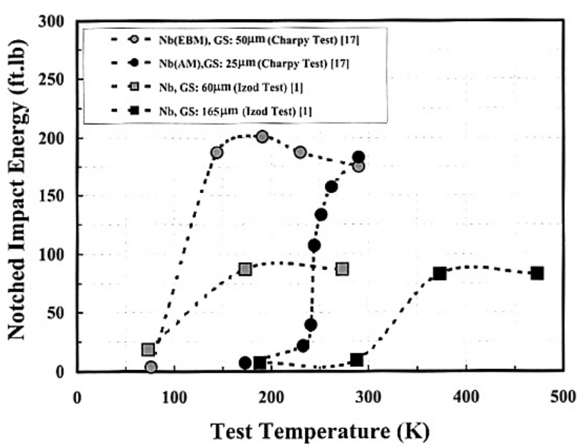

Figure 6. Effects of changes in grain size and processing conditions on impact energy and DBTT of Nb [12].

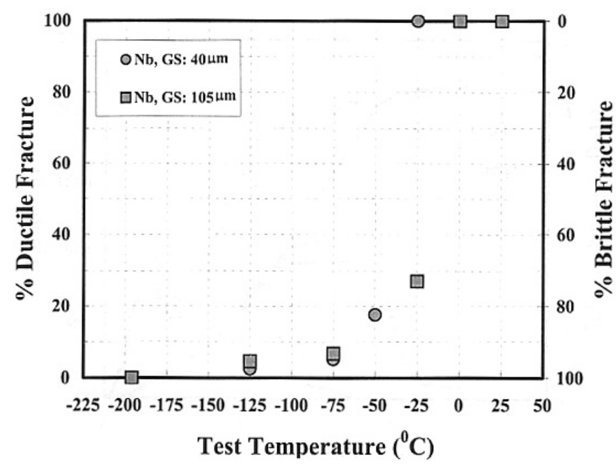

Figure 7. Effects of changes in grain size on DBTT and fracture surface appearance of Nb [22].

The competition between flow and cleavage fracture in polycrystalline Nb and Nb alloys (including Si-solid solution strengthened Nb) was investigated [14,16,17,22] where the cleavage fracture stress was measured via notched specimens. The results of those works

[14,16,17,22] revealed that cleavage fracture in polycrystalline Nb and Nb alloys occurs by reaching a temperature independent critical cleavage fracture stress. The magnitude of the cleavage fracture stress was shown to depend solely on the grain size in the materials studied, with decreases in grain size producing increases to the cleavage fracture stress [14]. The temperature independent values for cleavage fracture stress varied from 1000 – 1500 MPa depending on the grain size [14,16,17]. Extensive fractography of the notched bend specimens revealed that cleavage fracture initiated ahead of the notch in the region of peak tensile stress [14,16,17,22], entirely consistent with classic theories of tensile stress controlled cleavage fracture. The high constraint and stress levels present in the composites shown in Figure 5 indicate that cleavage of the refractory phase may occur in such systems.

The static fracture toughness of polycrystalline Nb has been determined on fatigue precracked bend specimens tested over temperatures ranging from 77K to 298K [23]. In addition, dynamic fracture toughness tests, K_{ID}, have been determined on fatigue precracked Charpy impact specimens tested in an instrumented impact machine [22]. The latter are shown in Figure 8 and reveal that the fracture toughness obtained under dynamic loading conditions is in the range 30-40 MPa-m$^{1/2}$ from 77K to above 298K, while fracture surface examination revealed the fracture to consist of 100% cleavage fracture [22-24]. The values obtained for the static fracture toughness over a more limited temperature range were in close agreement with the data obtained under impact conditions [14], suggesting that the minimum fracture toughness of the polycrystalline Nb samples is quite large (i.e. 30-40 MPa-m$^{1/2}$), despite the appearance of 100% cleavage fracture. More recent work [22,24] has indicated that R-curve (i.e. resistance curve) behavior may occur during cleavage of Nb and Nb alloys, depending on the test temperature and loading rate. In these cases, the appearance of cleavage fracture occurred with stable fracture under rising load conditions, producing an increase in toughness with increase in crack length despite the appearance of cleavage fracture. The fracture toughness of Nb-Si solid solution alloy was approximately 30 MPa-m$^{1/2}$ [16,17] at 298K.

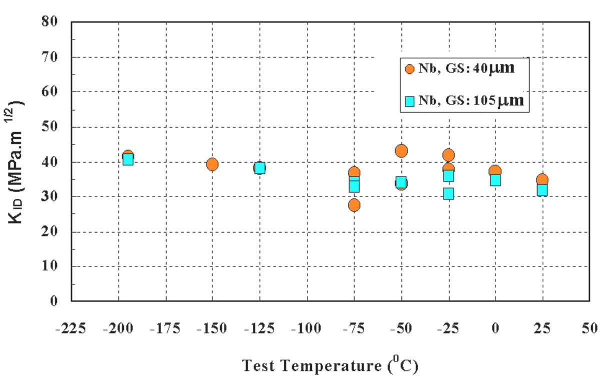

Figure 8. Grain size and test temperature effects on dynamic fracture toughness, K_{ID}, of Nb [24].

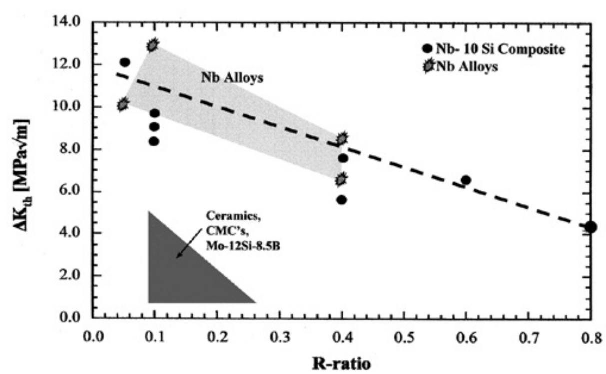

Figure 9. Summary of effects of changes in stress ratio on fatigue threshold of a variety of high temperature materials [3,13,25-30] tested at 298K.

The fatigue crack growth behavior of polycrystalline Nb has not been investigated to any great extent. Recent work [3,13,25-27] has revealed thresholds for fatigue in the range of 10-12 MPa-m$^{1/2}$ at R=0.1 at 298K. Paris Law slopes were in the range 2-4, consistent with most metallic materials. Increases in stress ratio decreased the fatigue threshold somewhat without significantly changing the Paris Law exponent, consistent with most metallic materials. This is shown in Figure 9 and includes data for some composites to be discussed below.

Fracture and Fatigue Behavior of Nb-Nb Silicide Composites

Composites based on the binary Nb-10 a/oSi system shown in Figure 10 have been extensively investigated. The majority of the work [1-3, 9-11,16,17,25-27] on this system has been conducted on arc cast/extruded material, subsequently heat treated 1500C/100 hrs in order to equilibrate the structure to contain Nb_5Si_3 and Nb (ss-Si). The structure shown in Figure 10 exhibits elongated primary Nb(ss-Si) present at about 50 volume %. The primary Nb has a grain size of roughly 25-50 μm, with the size of the primary Nb roughly 50-100 μm. Secondary Nb is present at about 25 volume % with a size of about 1 μm. The remaining 25% of the structure is the brittle Nb_5Si_3. More recent work has investigated alloy variants of this system where Hf, Ti, Cr, Ge, etc. have been added to change the balance of properties and oxidation resistance [3].

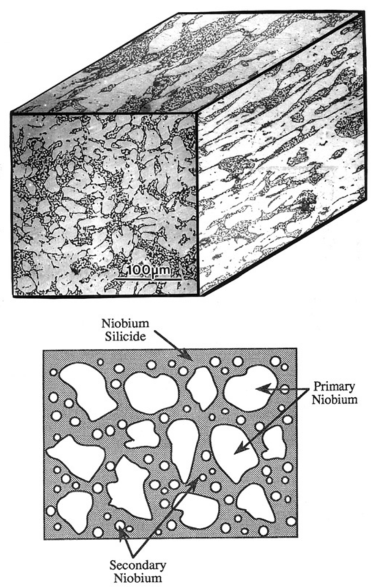

Figure 10. Typical microstructure of arc cast/extruded Nb-10 a/o Si alloy [9, 16].

Fracture toughness tests conducted on the monolithic Nb silicide revealed that it possessed a fracture toughness of only 1-2 MPa-$m^{1/2}$ [11]. Fracture toughness tests on the Nb-Si composite shown in Figure 10 were conducted so that crack growth occurred perpendicular to the extrusion direction. R-curve behavior and significant increases in toughness were exhibited by the Nb-Si composite due to the toughening provided by the Nb (ss-Si). Figure 11 presents a sequence of photographs taken at increasingly higher load (i.e. A-B-C-D) in a test conducted at 298K [32]. Cracks which have impinged on the Nb are blunted and the Nb deforms significantly before fracture. Figure 12 shows [3] the R-curve for a DS material of a multi-component system that arises due to the type of fracture processes shown in Figure 11.

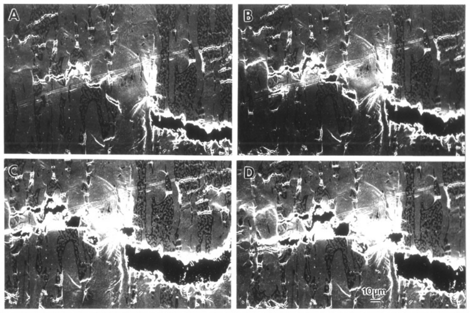

Figure 11. In-situ fracture experiment showing crack impingement on tough Nb in Nb-10 a/o Si composite increasing load from A-D [16,32].

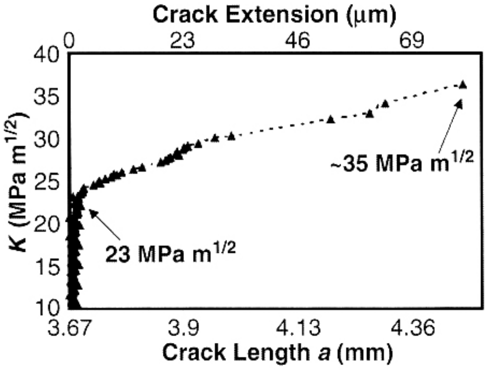

Fig. 12. Typical R curve of Nb silicide, showing an initiation toughness of 23 MPa $m^{1/2}$ and a peak toughness of ~35 MPa $m^{1/2}$. Similar behavior was observed in investment-cast Nb silicide [3].

Tests over a wider range of loading rates for the Nb-Si composite system are summarized in Figure 13 [16]. The toughness, roughly 24 MPa-$m^{1/2}$ is relatively insensitive to large changes in loading rate and test temperature. The very high levels of toughness exhibited at 77K at the fastest loading rates occurred with a preponderance of cleavage of the primary Nb in the composite [16]. Despite the presence of cleavage fracture of the primary Nb, the fracture toughness far exceeded that of the Nb silicide. This appears to be consistent with the high toughness of the polycrystalline Nb presented earlier (cf Fig. 8) despite the appearance of 100% cleavage. Testing at 773K does not significantly change the fracture toughness of the Nb-10 a/o Si composite or that of a variety of Nb-Ti-Si directionally solidified (DS) composites [3,31] despite a change in fracture mode of the toughening phase over that range of temperatures.

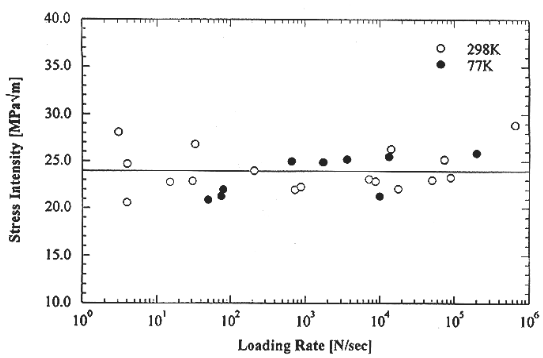

Figure 13. Effects of changes in loading rate and test temperature on toughness of Nb-10 a/o Si composite [16].

Exposure of the Nb-10 a/o Si system to oxygen at high temperature produced significant hardening and embrittlement of the Nb (ss-Si), thereby reducing the fracture toughness of the composite [32]. Recent alloying studies have produced significant increases to the oxidation resistance without significantly degrading the fracture and fatigue performance [2,3], as will be discussed below.

Few studies of the fatigue crack growth behavior of toughened Nb-Si composites have been conducted. Early work [33-35] on other Nb toughened intermetallics suggested that the fatigue performance of such toughened systems might be as poor as that of the monolithic brittle matrix, with Paris Law slopes approaching 100 in some cases. In those cases, the toughening constituent failed prematurely via fatigue [33-35]. In order to address the relevance of these issues for the Nb-Si system, extensive testing over a range of stress ratios and test temperatures has been conducted [3,25-28], followed by quantitative fractography in order to document the type of fracture mechanism(s) operating in the different fatigue regimes for the Nb-10 a/o Si composite shown in Figure 10.

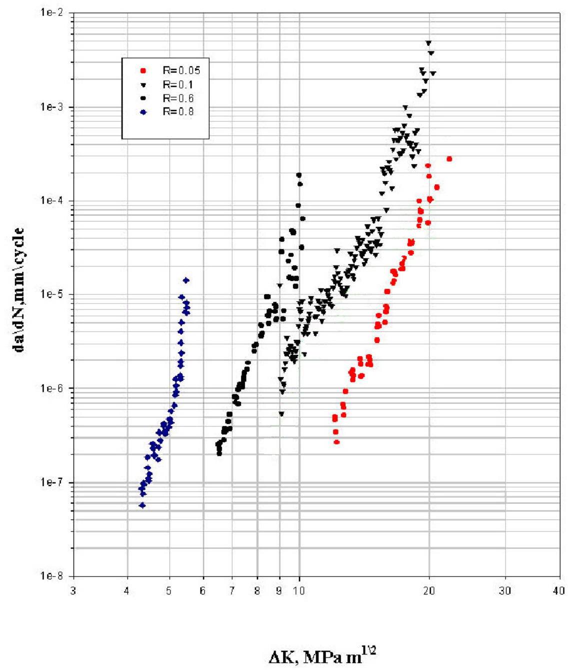

Figure 14. Effects of changes in stress ratio on fatigue of Nb-10 a/o Si composites.

Recent fatigue crack growth experiments at 298K on the Nb-10 a/o Si system [3,25-28] are summarized in Figure 14. Fatigue crack growth experiments were conducted on bend bar specimens tested at stress ratios ranging from 0.05 – 0.8 on a closed loop MTS servo-hydraulic testing machine. Crack growth was monitored via the use of foil resistance gages (i.e. KRAK gages) bonded to the outer surface of the specimens. Multiple tests were conducted for each stress ratio and representative results are shown in Figures 9 and 14. The fatigue threshold and Paris Law slope at R=0.1 is similar to that of metallic materials as shown in Table 1 and Figure 9. Figures 9, 14, and Table 1 also reveal that increasing the stress ratio decreases the fatigue threshold and increases the Paris Law slope. While the former observation (i.e. decreased fatigue threshold) is consistent with the behavior of metals [29], the increase in Paris Law slope with increasing stress ratio is typically not observed in monolithic metals. Initial work [25,26] revealed that cleavage fracture of the primary Nb occurred in the Paris Law regime of the Nb-10 a/o Si composites. Recent tests conducted over a wider range of stress ratios combined with quantitative fractography have determined the amount of cleaved primary Nb at different ΔK, as discussed below [28].

Table I – Fatigue crack growth behavior and toughness of Nb-Nb silicide composites

Materials	Processing Condition	R-ratio	ΔK_{th}, $MPa\text{-}m^{1/2}$	m–Paris Law Slope	K_{IC}, $MPa\text{-}m^{1/2}$
Nb-10Si	Extruded + HT	0.05	12	6.1	23.4*
	Extruded + HT	0.1	9	6.6	24.1*
	Extruded + HT	0.1	8.4	6.5	24.3*
	Extruded + HT	0.1	9.7	6.3	22.3*
	Extruded + HT	0.6	6.5	8.9	25.4*
	Extruded + HT	0.6	6	9.9	24.8*
	Extruded + HT	0.8	3.2	21.6	25.2*
	Extruded + HT	0.8	4.4	16.9	27.2*
Nb-15Si	Extruded +HT	0.1	4.4	6.4	20.6*
	Extruded +HT	0.4	4.1	-	-
	Extruded +HT	0.6	4	5.6	22.5*
	Extruded +HT	0.8	3.7	-	24.9*
Nb-12Si	DS	0.1	13.2	16.7	18.1
Nb-18.2Si	DS	0.1	2.5	-	3.3
Nb-30Ti-8Cr-10Al-14Si	DS	0.1	-	-	8.3**
Nb-42.5Ti-15Si	DS	0.1	5.5	9.7	10.2
Nb-Ti-Hf-Cr-Al-Si	DS	0.1	8.5	2.9	24.2
Nb-22Ti-3Hf-2Cr-2Al-17Si	Extruded +HT	0.1	7.1	4.8	24.4
	(1500°C/100hr)	0.4	5.6	4.1	19.8
Nb-22Ti-3Hf-2Cr-2Al-17Si	Extruded +HT	0.1	7.2	4.8	17.8
	(1400°C/100hr)	0.4	3.9	4.2	13.9
Nb-22.5Ti-6Cr-3Fe-2Hf-12.5Si-2Al-5Ge-1.2Sn	Extruded	N/A	N/A	N/A	8.6, 6.0 **
Nb-19.5Ti-13Cr-2Hf-17.5Si-2Al-1.2Sn	Extruded	N/A	N/A	N/A	10.1, 10.1**
Nb-21.5Ti-9Cr-2Hf-17.5Si-2Al-1.2Sn	Extruded	N/A	N/A	N/A	10.6**
Nb-22.5Ti-6Cr-3Fe-2Hf-12.5Si-2Al-5Ge-1.2Sn	Extruded	N/A	N/A	N/A	9.5, 9.3**

* K_{max} at fatigue overload **Without precracking

It is clear [25-28] that increases in ΔK increase the amount of cleaved primary Nb. However, as shown earlier in this review, cleavage of Nb is typically considered a static fracture mode controlled by reaching a critical value of the cleavage fracture stress [14]. If this is the case, cleavage during fatigue crack growth should be controlled by K_{max} in the fatigue loading cycle. Figure 15 plots the observation of cleavage on the fatigue fracture surface of Nb-Si composite materials at different values of K_{max} instead of ΔK [25-28]. The use of Kmax appears to normalize all of the data obtained at different stress ratios at 298K and suggests strongly that the increase in the Paris Law slope exhibited in Figure 13 and Table 1 with increasing stress ratio is due to the intervention of static modes of fracture (i.e. cleavage) in the primary Nb. Recent work [36] on steels has revealed similar observations of increasing R producing increased Paris Law slopes in combination with an increased occurrence of cleavage fracture on the fatigue fracture surfaces. This further suggests that microstructure manipulation and/or testing at different temperatures could affect the tendency for cleavage of the primary Nb, and hence significantly change the fatigue crack growth characteristics. Preliminary work of this nature has produced fatigue crack growth characteristics and fractographic observations which are consistent with these predictions [28].

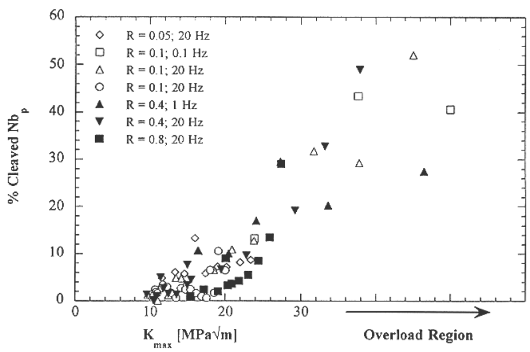

Figure 15. Quantitative fractography results showing an increase in amount of cleaved primary Nb with increasing K_{max} in Nb-10 a/o Si composites.

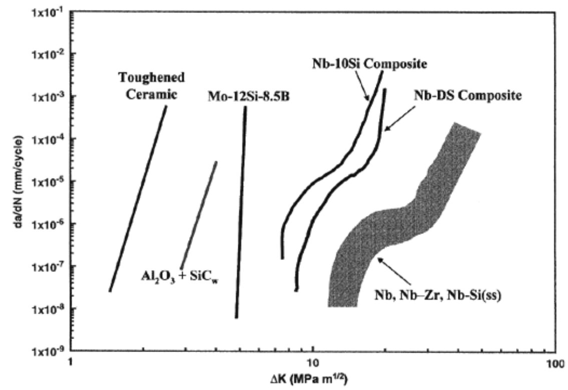

Figure 16. Comparison of fatigue behavior of some high temperature materials [25-30].

Higher alloy variants of the Nb-10 a/o Si system have been prepared in order to improve the oxidation resistance [2,3]. Both arc-casting/extrusion as well as DS materials have been prepared. Table 1 also summarizes the fatigue threshold and Paris Law slope of the materials prepared and tested to date [3,27,28]. It is again clear that these Nb alloy toughened composites can exhibit fatigue thresholds, Paris Law exponents, and values for fracture toughness which are metallic-like in character. In order to demonstrate this, Figures 9 and 16 were prepared from the data obtained presently as well as that taken from the literature [29,30]. Included in Figures 9 and 16 are data for ceramics, toughened ceramics, ceramic composites, and preliminary work on Mo based intermetallic composites. The fatigue thresholds are as low as 1.5 MPa-$m^{1/2}$ at R=0.1, with Paris Law slopes for these other systems approaching 60 - 100 in some cases [29,30], in contrast to the high threshold and low Paris Law slope (i.e. <10) values generally exhibited by the Nb-Si system at R=0.1. Although the Nb toughened Nb Silicide composites exhibit an increase in Paris Law slope with increased stress ratio, this is apparently due to the intervention of static modes of fracture during the fatigue test. Reducing the tendency for the Nb phase(s) to cleave via microstructure changes, or testing at higher temperatures, should further improve the Paris Law slope of the Nb-Si systems.

Flow and Fracture of Bulk Metallic Glass Composites

Metallic glasses represent a class of materials with exceptionally high strength, good corrosion resistance, good magnetic properties, and combinations of properties not generally available with conventional structural materials [4,5,38]. The lack of crystalline structure produces materials with near theoretical strength, in the range 2-4 GPa, depending on the composition of the glass [37]. Recent work on the monolithic bulk metallic glasses [4,5,38-44] has investigated the strength/toughness combinations possible in these materials. While the strength/toughness combinations are impressive in such systems, the lack of crystalline structure produces a failure mechanism at 298K which occurs via the initiation and propagation of locally intense shear. This process severely limits the tensile ductility, with most bulk glasses exhibiting zero tensile ductility. However, the incorporation of crystalline regions of a Nb containing phase has been shown to increase the tensile ductility [4,6-8] without significantly degrading the strength. Figure 17 shows the microstructure of a bulk metallic glass composite which contains a crystalline Nb-Ti-Zr phase in an amorphous matrix [4,6-8]. The dendritic structure of the crystalline phase is produced via controlled devitrification during cooling of the metallic glass.

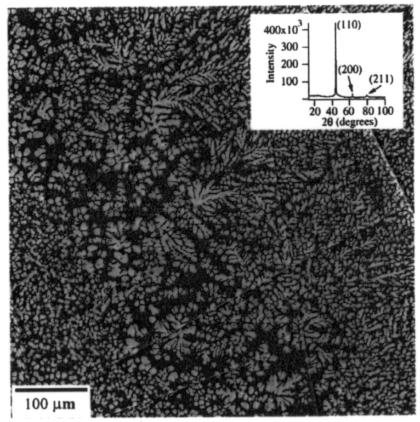

Figure 17. Bulk metallic glass composite containing a Nb-Ti-Zr crystalline phase designed to impart enhanced ductility and toughness [4,6-8].

The beneficial role of the Nb containing phase in the metallic glass composites appears to be through its ability to block shear bands. This promotes the evolution of more shear bands along with deformation of the Nb containing phase, thereby increasing the tensile ductility. The Nb phase experiences very high constraint in these composites due to the large mismatch in properties between the amorphous and crystalline phase. Thus, understanding the flow and fracture behavior of Nb and Nb alloys is extremely relevant to the design of optimized composite microstructures. Changes to the Nb alloy grain size, alloy content, etc. will likely have large effects on the balance of properties possible in the metallic glass composites.

Much less work has been done to characterize the fracture and fatigue behavior of the metallic glass composites, although considerable work has documented the flow and fracture behavior of the bulk metallic glass matrix, as summarized elsewhere [4,5, 38-43]. Very recent work has compared the fatigue precracked fracture toughness of the bulk metallic glass to that of the bulk metallic glass composite with the Nb containing crystalline phase [5]. Figure 18 shows the effects of changes in test temperature on the fracture toughness of the bulk metallic glass as well as the composite. It is clear that the addition of the Nb containing phase provides significant increases to the fracture toughness of the bulk metallic glass, while the magnitude of the improvement appears to be temperature dependent. In Figure 18, the fracture toughness of the composite is highest at the highest test temperature and lowest at the lowest test temperature. In contrast, the fracture toughness of the bulk metallic glass matrix is relatively insensitive to changes in test temperature over the range tested. The source of the temperature effect on the toughness of the bulk metallic glass composite appears to be due to the behavior of the Nb containing phase [5]. At the highest test temperatures, the Nb phase deforms and fractures via a ductile fracture mechanism with significant shear banding of the metallic glass matrix. In contrast, at the lowest test temperatures, a larger fraction of the Nb phase fails via cleavage fracture, with somewhat less shear banding of the metallic glass matrix. Additional work is focusing on the fatigue crack growth behavior of such composites in comparison to the bulk amorphous matrix [44].

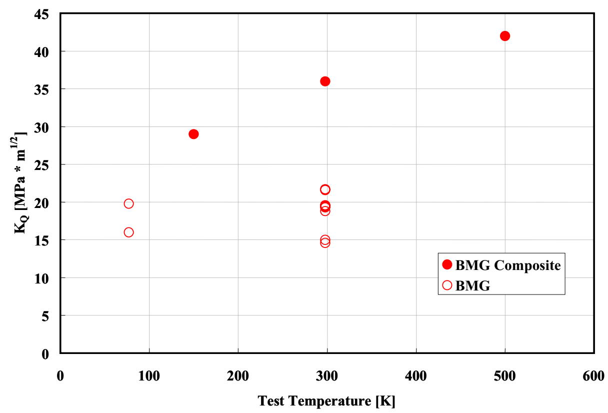

Figure 18. Effects of changes in test temperature on fracture toughness of a bulk metallic glass and bulk metallic glass composite containing a Nb-Ti-Zr crystalline phase [5].

It is clear that the incorporation of Nb containing phase(s) can provide significant benefits to the balance of properties in some of the bulk amorphous metals. Much work remains to be done in order to understand the role of the Nb phase(s) in promoting shear banding. Optimization of the composite properties will require a thorough investigation of the factors controlling the flow and fracture of the Nb phase(s) as well as their behavior in the presence of a metallic glass matrix which presents a large mismatch in properties.

Summary

The data obtained to date indicates that it is important to investigate the behavior of the monolithic toughening phase(s) in order to understand their role in the toughening and fatigue behavior of composites based on silicides as well as bulk metallic glasses. Further work is clearly necessary in order to demonstrate that alloying additions to the high temperature silicide composites are effective in improving the oxidation resistance without negatively impacting the properties. The issues in the metallic glass composites relate to optimization of the Nb phase(s) for ductility and toughness enhancement and significant work remains to be done in this and related areas. In addition, there is virtually no data on the high cycle fatigue and small crack growth behavior of such systems. Additional fatigue tests at different temperatures and stress ratios are also needed to determine the generality of the arguments presented here.

Acknowledgments

The authors would like to acknowledge the work and help of a number of former and present students: JD Rigney, J Kajuch, J Short, WA Zinsser, A Samant, A Awadallah, PM Singh, L Leeson, L Ludrosky, J Larose, D Padhi, P Lowhaphanudu, AK Thurston, and S. Solv'yev. Useful discussions with D Dimiduk, B Bewlay, M Jackson, M Mendiratta, J Larsen, RO Ritchie, AW Thompson, and WL Johnson are acknowledged. Supply of materials by M Mendiratta, B Bewlay, WL Johnson, A Peker, ATI, Inc., and Liquidmetal Inc. are appreciated as is funding by Reference Metals Co., Howmet, GE-CRD, MTS Systems, AFOSR- F49620-96-1-0164, AFOSR-F49620-00-1-0067, AFOSR-AASERT F49420-96-1-0228, DARPA SAM via ARO-DAAD19-01-1-1525.

References

1. DM Dimiduk, MG Mendiratta, and PR Subramanian, in ISSI-I Structural Intermetallics, (R Darolia et al eds.), TMS, Warrendale, PA, (1993) 619-630.
2. BP Bewlay, JJ Lewandowski, and MR Jackson, JOM, August, (1997) 44-47.
3. BP Bewlay, MR Jackson, JC Zhao, PR Subramanian, MG Mendiratta, and JJ Lewandowski, MRS Bulletin, 28(9) (2003) 646-653.
4. WL Johnson: MRS Bulletin., 24 (1999) 42-56.
5. JJ Lewandowski, AK Thurston, and P Lowhaphandu, MRS Proceedings - Vol. 754 (T. Egami, et al eds.) MRS, Warrendale, PA (2003) 307-315.
6. RD Conner, H Choi-Yim, and WL Johnson, J Mater. Res.14 (1999) 3292-3297.
7. RD Conner, RB Dandliker, and WL Johnson, Acta Mater. 46 (1999) 6089-6102.
8. H Choi-Yim, RD Conner, F. Szuecs, and WL Johnson, Scripta Mater., 45 (2001) 1039-1045.
9. MG Mendiratta, JJ Lewandowski, and DM Dimiduk, Metall. Trans. A, 22A (1990) 1573-1583.
10. MG Mendiratta and DM Dimiduk, Metall. Trans. A, 24A (1993) 501-504.
11. J Kajuch, JW Short, and JJ Lewandowski, Acta Metall. et Materialia, 43 (1995) 1955-1967.
12. D Padhi, Ph.D. Thesis, Case Western Reserve University, Dept. Materials Science and Engineering, January 2001.
13. JJ Lewandowski, D Padhi, and S Solv'yev, in ISSI-III Structural Intermetallics, (K. Hemker et al eds.) TMS, Warrendale, PA, (2001) 371-380.
14. A Samant and JJ Lewandowski, Metall. Trans. A, 28A (1997) 389-399.
15. MA Adams, AC Roberts, and RE Smallman, Acta Metall., 8 (1960) 328-337.
16. JD Rigney and JJ Lewandowski, Metall. Trans. A, 27A (1996) 3292-3306.
17. MG Mendiratta, R Goetz, DM Dimiduk, and JJ Lewandowski, Metall. Trans. A, 26A (1995) 1767-1777.
18. PR Subramanian, MG Mendiratta, DM Dimiduk, and MA Stucke, Mater. Sci. Eng., A239-240 (1997) 1.
19. BP Bewlay, MR Jackson, and HA Lipsitt, Metall. and Materials Trans. A, 27A (1996) 3801.
20. MR Jackson and KD Jones, in Refractory Metals: Extraction, Processing, and Applications, (KC Liddell, DR Sadoway, and RG Bautista, eds.), TMS, Warrendale, PA, (1990) 335.
21. MG Mendiratta, JJ Lewandowski, and DM Dimiduk, Metall. Trans. A, 22A (1991) 1573-1583.
22. D. Padhi and JJ Lewandowski, Metall Trans A, 34A(4) (2003) 967-975.
23. A Samant and JJ Lewandowski, Metall. Trans. A, 28A (1997) 2297-2307.
24. D Padhi and JJ Lewandowski, Materials Science and Engineering A, (2003) in press.
25. WA Zinsser and JJ Lewandowski, Scripta Metall. et Materialia, 38(12) (1998) 1775-1780.
26. WA Zinsser and JJ Lewandowski, Metall. Trans. A, 29A (1998) 1749-1757.
27. JJ Lewandowski, in Fatigue '99, (XR Wu and ZG Zhang, eds.), Volume III, EMAS (1999) 1471-1477.
28. S Solv'yev and JJ Lewandowski, Unpublished Research, Case Western Reserve University, Cleveland, OH (2000).
29. RO Ritchie, Intl Journal Fracture, 100 (1999) 55-83.
30. H Choe, D Chen, JH Schneibel, and RO Ritchie, in Fatigue and Fracture of High Temp. Matl's, (PK Liaw , ed.), TMS Warrendale, PA (2000) 17-24.

31. JD Rigney, BP Bewlay, DM Dimiduk, and JJ Lewandowski, Unpublished Research, (1998).
32. JD Rigney, PM Singh, and JJ Lewandowski, JOM, August (1992) 36-41.
33. KTV Rao and RO Ritchie, Mater. Sci. Eng. A153 (1992) 479-485.
34. KTV Rao, WO Soboyejo, and RO Ritchie, Metal. Trans. A, 23A (1992) 2249-2257.
35. WO Soboyejo and SML Sastry, Mater. Sci. Eng. A171 (1993) 95-104.
36. AB El-Shabasy and JJ Lewandowski, Int'l Journal Fatigue, (2003), in press.
37. P Wesseling, P Lowhaphandu, and JJ Lewandowski, MRS Proceedings - Vol. 754 (T. Egami, et al eds.) MRS, Warrendale, PA (2003) 281-287.
38. JJ Lewandowski, Mater Trans JIM, 42(4),(2001) 633-637.
39. JJ Lewandowski and P Lowhaphandu, Philos Mag A 82(17/18) (2002) 3427-3441.
40. P Lowhaphandu, SL Montgomery, and JJ Lewandowski, Scripta Mater 41(1) (1999) 19-24.
41. P Lowhaphandu, LA Ludrosky, SL Montgomery, and JJ Lewandowski, Intermetallics 8 (2000) 487-492.
42. P Lowhaphandu and JJ Lewandowski, Scripta Mater 38(12) (1998) 811-1817.
43. RD Conner, AJ Rosakis, WL Johnson and DM Owen, Scripta Mater, 37 (1997) 1373-1379.
44. AK Thurston, S Solv'yev, and JJ Lewandowski, Unpublished Research, Case Western Reserve University, Cleveland, OH (2003).